Acta Phys. Hung. A 19/1 (2004) 000–000

HEAVY ION PHYSICS

From multifragmentation to supernovae and neutron stars

Ph.Chomaz[1], F.Gulminelli[2,a], C.Ducoin[1,2], P.Napolitani[1] and K.Hasnaoui[1]

[2] GANIL (DSM - CEA / IN2P3 - CNRS), B.P.5027,
F-14076 Caen Cédex 5, France[1] LPC Caen (IN2P3 - CNRS / EnsiCaen et Université),
F-14050 Caen Cédex, France

Received 1 January 2004

Abstract. The thermodynamics properties of globally neutral dense stellar matter are analyzed both in terms of mean field instabilities and structures beyond the mean field. The mean field response to finite wavelenght fluctuations is calculated with the realistic Sly230a effective interaction. A Monte Carlo simulation of a schematic lattice Hamiltonian shows the importance of calculations beyond the mean field to calculate the phase diagram of stellar matter. The analogies and differences respect to the thermodynamics of nuclear matter and finite nuclei are stressed.

Keywords: Dense matter; Compact stars; Liquid-gas phase transition; Multifragmentation
PACS: 68.35.Rh, 26.60.+c

1. Introduction

Supernovae explosions, powered by the release of gravitational energy of a massive star which has exhausted its nuclear fuel, can lead to the formation of a most interesting dense stellar object: a neutron star[1]. Due to the lack of observational data, the composition and structure of a neutron star is still highly hypothetical[2]. In the outer part of the star, the stellar crust extending over about one kilometer, the matter density is expected to be comparable to normal nuclear matter density, and the star can be modelized as essentially composed of neutrons, protons, electrons and neutrinos in thermal and chemical equilibrium. In a few minutes after its birth, the proto-neutron star formed at a temperature of $\approx 10^{11} K$ becomes transparent to neutrinos and cools via neutrino emission to temperatures which are small on

1219-7580/04/ $ 20.00

the nuclear scale. The cooling process occurs via heat conduction and convection through the envelope to the surface on a time scale too short for the system to be in global thermal equilibrium, however local thermal equilibrium should be well verified during the whole evolution of the proto-neutron star, and beta-equilibrium is also often assumed[3]. Crust matter is therefore very similar to nuclear matter, which is known to exhibit a complex phase diagram including first and second order phase transitions[4, 5] .

The analogy between stellar matter and nuclear matter hides however an important difference. If nuclear matter is by definition neutral, only global charge neutrality is required by thermodynamic stability for stellar matter. An important consequence of the charge neutrality constraint is that the canonical free energy density f is defined only for $\rho_c = \rho_p - \rho_e = 0$. Hence $f\left(T, \rho_n, \rho_p, \rho_e\right) = f\left(T, \rho_n, \rho\right)$ with $\rho = (\rho_p + \rho_e)/2$ and the chemical potential μ_c associated to ρ_c can not be defined since the free energy is not differentiable in the total-charge direction[2]. This constraint affects the thermodynamics directly since it changes the number of degrees of freedom of the thermodynamic potentials[6]. These considerations are expecially relevant when phase transitions are concerned. For exemple, since μ_c is not a thermodynamic variable, the coexistence condition between two phases A and B $\mu^A = \mu^B$ does not imply that each of the chemical potentials μ_e and μ_p are identical in the two phases . The difference in chemical potentials of charged particles is counterbalanced by the Coulomb force: as some electrons move from one phase to the other driven by the chemical-potential difference, the Coulomb force reacts forbidding a macroscopic charge to appear.

2. Mean Field approximation

To illustrate the consequence of charge neutrality for the phase diagram of stellar matter, we present mean field calculations[7] using the Sly230a effective interaction, which has been optimized to describe exotic nuclei and pure neutron matter[8]. This force has been already applied to neutron stars crust in ref.[9].

2.1. Homogeneous matter

The matter instability to density fluctuations can be spotted looking at the curvature matrix[10]

$$C = \begin{pmatrix} \partial\mu_n/\partial\rho_n & \partial\mu_n/\partial\rho_p \\ \partial\mu_p/\partial\rho_n & \partial\mu_p/\partial\rho_p + \partial\mu_e/\partial\rho_e \end{pmatrix} , \tag{1}$$

where the free energy density is $f(T, \rho_n, \rho) = f_N(T, \rho_n, \rho_p = \rho) + f_e(T, \rho_e = \rho)$, and we have introduced the chemical potentials $\mu_n = \partial f_N/\partial\rho_n$, $\mu_p = \partial f_N/\partial\rho_p$ and $\mu_e = \partial f_e/\partial\rho_e$. The additional term $\chi_e^{-1} = \partial\mu_e/\partial\rho_e$ in the matrix modifies the stability conditions with respect to to the nuclear matter part, i.e. to the curvature of f_N. Due to the small electron mass, i.e. high Fermi energy, the electron fluid is highly

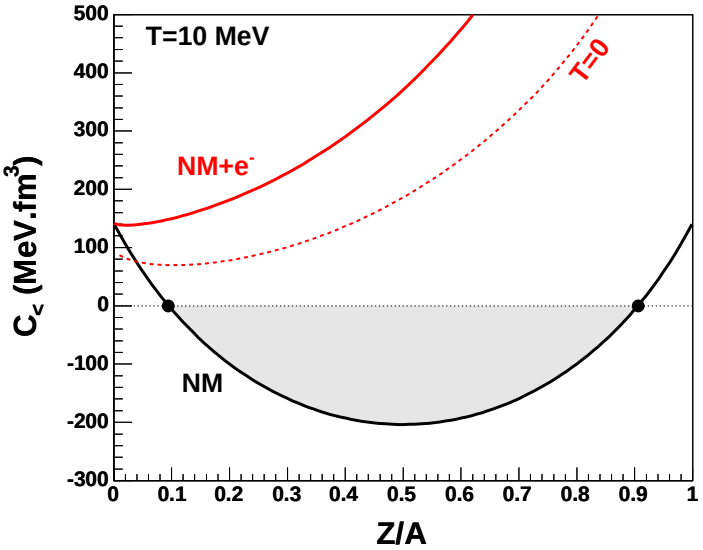

Fig. 1. Minimum curvature of the mean field free energy matrix as a function of isospin asymmetry for normal nuclear matter(NM) and for stellar matter (NMe) at a temperature $T = 10MeV$ calculated with the Sly230a effective interaction. Dashed line: stellar matter at zero temperature.

incompressible leading to a quenching of the instability: the instability conditions $\mathrm{Det}\, C \leq 0$ or $\mathrm{tr}\, C \leq 0$ are more difficult to fulfill. The result for the Sly230a interaction is shown in Figure 1: the lowest eigenvalue of the curvature matrix is always positive independent of the temperature and proton fraction, meaning that the spinodal zone is suppressed in stellar matter[7].

2.2. Finite wavelenght fluctuations

If we expect stellar matter to be stable at all temperatures respect to global density fluctuations, it is well known that the matter ground state in the inner crust should correspond to clusterized solid configurations composed of finite nuclei on a Wigner lattice[11]. To access these inhomogeneous configurations, stellar matter may be instable respect to finite wavelenght density fluctuations, $\delta\rho_q = A_q e^{i\vec{k}\cdot\vec{r}} + A_q^* e^{-i\vec{k}\cdot\vec{r}}$, with $q = n, p, e$. The mean field response to such a fluctuation induces two extra terms in the curvature matrix eq.(1)[10]. The gradient term of the Skyrme fonctional[8] produces a term $\propto k^2$ coupling proton and neutron densities, which tends to suppress high k fluctuations; the direct Coulomb interaction produces a term $\propto k^{-2}$ coupling proton and electron densities, which tends to suppress low k fluctuations. The resulting effect is the appearence of a finite k interval where one eigenvalue turns negative, i.e. matter becomes unstable. An exemple is shown in Figure 2[7]. We can see that an important instability region exists even at high temperatures and almost independent of the effective interaction employed, sug-

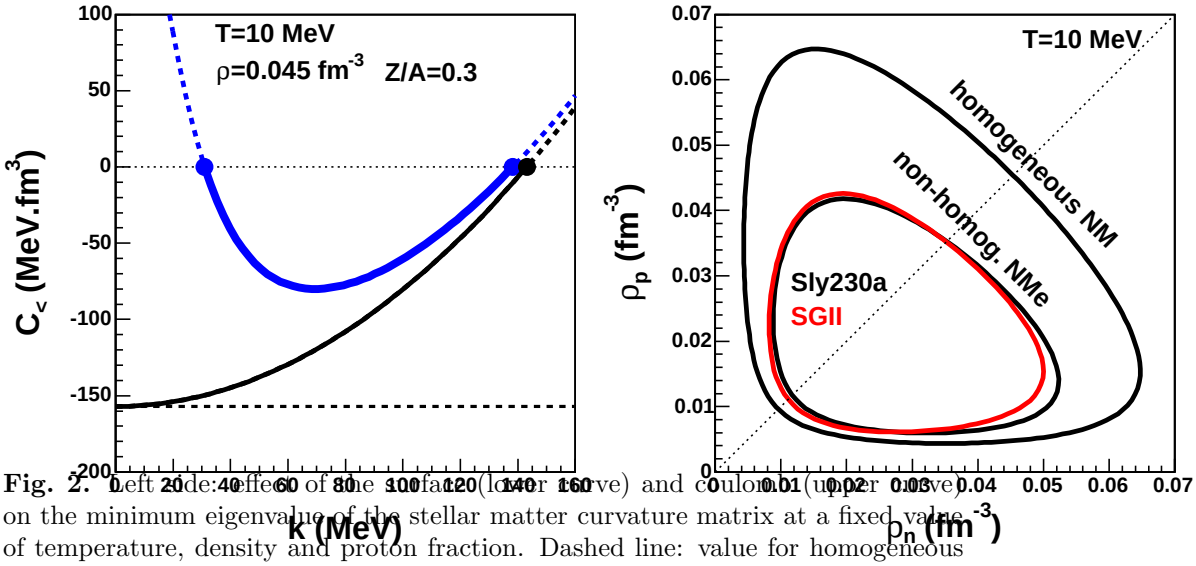

Fig. 2. Left side: effect of the surface (lower curve) and coulomb (upper curve) on the minimum eigenvalue of the stellar matter curvature matrix at a fixed value of temperature, density and proton fraction. Dashed line: value for homogeneous nuclear matter. Right side: instability region of homogeneous nuclear matter and inhomogeneous matter with electrons with two different effective interactions.

gesting that clusterized configurations may be important also in the proto-neutron star evolution.

2.3. The constraint of β-equilibrium

If the cooling time scale is sufficiently slow, the proto-neutron star will also be subject to the constraint of β-equilibrium, $\mu_p^{tot} + \mu_e^{tot} = \mu_n^{tot} + \mu_\nu$, with $\mu_q^{tot} = \mu_q + m_q$[12]. This is certainly the case in the final step of the star evolution, when the temperature is low enough for the matter to be completely transparent to neutrino emission, $\mu_\nu = 0$, which becomes then the most effective cooling process of the star[1]. Chemical equilibrium is generally assumed in the thermodynamic studies of stellar matter[10, 9] and is often assimilated to charge neutrality. However we would like to stress that chemical equilibrium, as well as any other other transformation like constant proton fraction or constant temperature, is just a restriction of the accessible states and does not affect the thermodynamic properties, which are state functions[13].

The chemical equilibrium constraint defines an accessible region in the phase diagram shown for a given temperature in Figure 3[7]. The lower limit is given by the equation $\mu_\nu = 0$ while lepton number conservation defines an upper limit. We can see in Figure 3 that, depending on μ_ν, i.e. on the neutrino opacity, the instability region can be crossed under the constraint of chemical equilibrium.

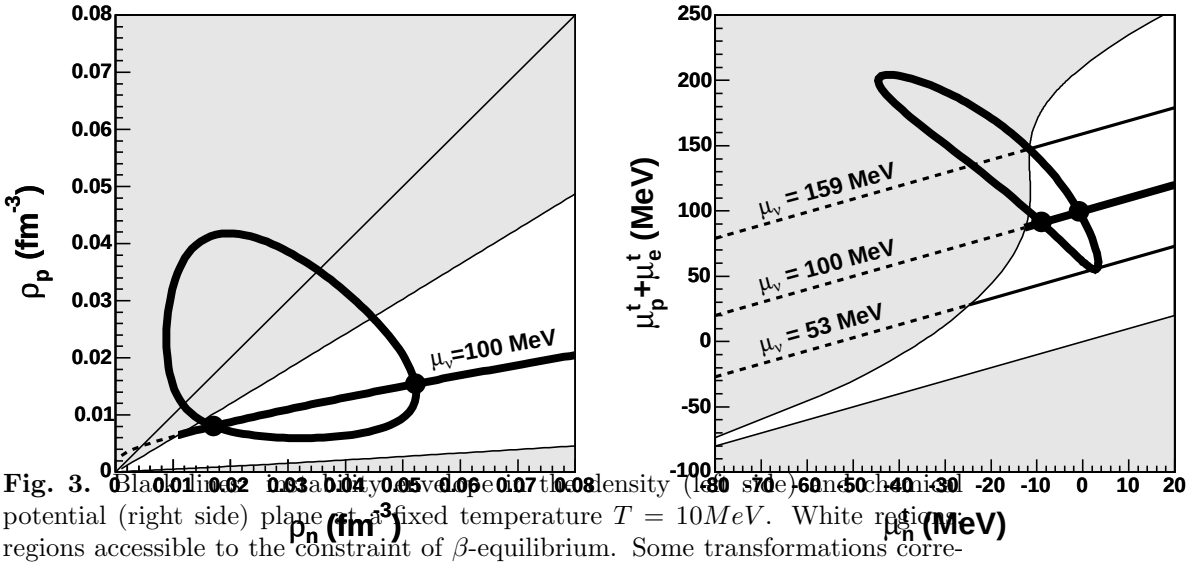

Fig. 3. Black line: instability region in the density (left side) and chemical potential (right side) plane at a fixed temperature $T = 10MeV$. White regions: regions accessible to the constraint of β-equilibrium. Some transformations corresponding to different neutrino chemical potentials are also given.

3. Coulomb frustration beyond the mean field

In the previous section we have seen that hot stellar matter can show an instability respect to finite wavelenght density fluctuations, eventually leading to the formation of clusterized configurations. This instability is due to the interplay between the surface and coulomb interaction terms. This effect is a specific application of the generic physical concept of frustration. Frustration occurs in condensed matter physics whenever interactions with opposite signs act on a comparable lenght scales; applications range from magnetic systems to liquid crystals, from spin glasses to protein folding[14]. A well known application of frustration in nuclear physics is given by the multifragmentation observed in violent ion collisions. Concerning compact stars, it is recognized since a long time that in the clusterized state generated by frustration the structures may abandon spherical shapes and organize according to more complex topologies (pasta phases) [15]. The possible survival of these structures at high temperature is discussed in the recent literature[16, 17].

3.1. A statistical treatment of frustration

A statistical tool to deal with frustrated systems is given by the multi-canonical ensemble[18]. The two energy components E_N, E_C are treated as two independent observables associated to two Lagrange multipliers β_N, β_C. A generalized grand potential is defined by

$$Z_{\beta_N,\beta_C,\vec{\alpha}} = \int d\vec{N} Z^c_{\beta_N,\beta_C}(\vec{N}) exp\left(-\vec{\alpha}\cdot\vec{N}\right) , \qquad (2)$$

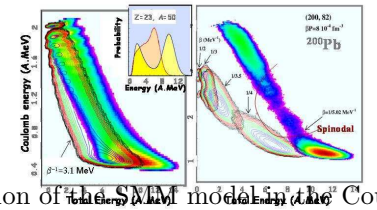

Fig. 4. Event distribution of the SMM model in the Coulomb energy versus total energy plane for a finite nucleus of atomic number $Z = 23$ (left part) and $Z = 82$ (right part) in the multi-canonical ensemble. Contour plots: uncharged system $\beta_C = 0$; contour lines: charged system $\beta_C = \beta_N$ with different values of β_N. Full line: spinodal curve. Insert: projection over the total energy axis for the uncharged (bimodal distribution) and the charged (monomodal distribution) case.

where e^{α_q} is the fugacity of particle type q and the multi-canonical partition sum reads

$$Z^c_{\beta_N,\beta_C}(\vec{N}) = \int dE_N dE_C W(E_N, E_C, \vec{N}) exp\left(-\beta_N E_N - \beta_C E_C\right) . \qquad (3)$$

If E_C represents the Coulomb energy and E_N the nuclear term, the choice $\beta_C = \beta_N$ gives the usual (grand)canonical thermodynamics for charged systems, $\beta_C = 0$ leads to the uncharged thermodynamics, while all intermediate values $0 < \beta_C < \beta_N$ correspond to interpolating ensembles, or equivalently to physical systems with an effective charge $(q_{eff}/q_0)^2 = \beta_C/\beta_N$. The multi(grand)canonical ensemble allows to construct a single unified phase diagram for neutral and charged matter, and is therefore an ideal statistical tool to make some connections between nuclear and stellar matter.

3.2. Application to multifragmentation

As an example let us consider the phenomenon of multifragmentation as modelized in the Statistical Multifragmentation Model[18]. The event distribution in the multi-canonical ensemble eq.(3) is represented in Figure 4 for a value β_N corresponding to the transition temperature for the uncharged case. The first order phase transition gives rise to a two peaked distribution in the (multi)canonical ensemble, representing the two coexisting phases. The direction separating the two

peaks can be taken as a definition of the order parameter [19]. From the left part of Fig.4 we can see that the effect of the Coulomb interaction is a rotation of the order parameter which becomes almost orthogonal to the total energy direction, leading to a reduction of the latent heat and a shrinking of the coexistence zone. When the Coulomb effect becomes important (right part), the spinodal region is not explored by the charged system and the phase transition becomes a cross-over.

3.3. An Ising based model of stellar matter

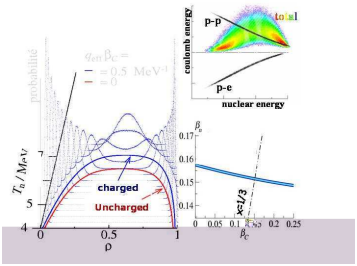

Fig. 5. Upper right: typical low temperature event distribution of the long ranged globally neutral Ising model. The proton-proton, proton-electron, and total distributions are given. Left: coexistence region for the uncharged and charged case obtained from the multi-grand-canonical particle number distributions. Lower right: phase diagram. The constant proton fraction $x = 1/3$ line is also shown.

To get a qualitative information of the effect of frustration on dense globally neutral stellar matter we have introduced a schematic but exactly solvable Ising model with long Coulomb-like and short nuclear-like range interactions[20]

$$H_N = -\frac{\epsilon}{2}\sum_{<ij>} n_i n_j \;\; ; \;\; H_C = \frac{\chi}{2}\sum_{i\neq j}\frac{q_i q_j}{r_{ij}} = \frac{\chi}{2}\sum_{i\neq j} n_i n_j C_{ij}\,, \tag{4}$$

where each site of a three dimensional lattice of $N = L^3$ sites is characterized by an occupation number $n_i = 0, 1$ and an effective charge $q_i = n_i - \sum_{j=1}^{N} n_j/N$. The effective charge represents the proton distribution screened by an uniform electron background[21]. To accelerate thermodynamic convergence, the finite lattice is repeated in all three directions of space a large number N_R of times

$$H_C^{tot} = \frac{\chi}{2} \sum_{n=1}^{N_R} \sum_{i,j}^{N} n_i n_j C_{IJ} \tag{5}$$

with $\vec{I} = \vec{i} + \vec{n}L$, $\vec{J} = \vec{j} + \vec{n}L$.

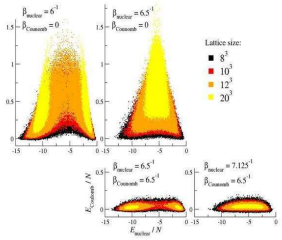

Fig. 6. Event distribution of the long ranged globally neutral Ising model in the Coulomb energy versus nuclear energy plane for different values of the Lagrange multipliers and different lattice sizes.

The resulting phase diagram is shown in Figure 5. We can see that, at variance with the case of multifragmentation of finite charged nuclei, the effect of the Coulomb interaction is an expansion of the coexistence zone. This result can be easily understood inspecting the event distributions in the multicanonical ensemble in Fig.5[20]. We can see that the proton-proton and proton-electron energy distributions are opposite in sign and similar in shape; in fact they would be exactly identical in the mean field approximation, meaning that the only effect of the charge at the mean field level is the addition of the electron free energy as we have discussed in section 2. The sum of the two contributions in this exactly solved model gives a two peaked distribution indicating coexistence between a high nuclear energy liquid and a low nuclear energy gas. The electron screening effect minimizes the Coulomb energy of the dense phase, making it accessible even at high temperature at variance with the finite nucleus case. This result implies that pasta phases may be relevant in a wide range of thermodynamic conditions .

Another important effect of the Coulomb interaction in stellar matter is to suppress the critical point of neutral nuclear matter and the related phenomenon

of critical opalescence. The Coulomb energy density can be expressed as

$$\frac{\langle \hat{V}_c' \rangle}{V} = \frac{\alpha}{2V} \int \frac{\sigma_c(\mathbf{r}, \mathbf{r}')}{|\mathbf{r} - \mathbf{r}'|} \mathrm{d}\mathbf{r}\mathrm{d}\mathbf{r}' = 2\pi\alpha \int \sigma_c(r) r \mathrm{d}r \ , \tag{6}$$

where $\sigma(\mathbf{r}, \mathbf{r}') = \langle \delta\rho_c(\mathbf{r}) \delta\rho_c(\mathbf{r}') \rangle$ is the charge density fluctuation. At the critical point $\sigma_c(r)$ is expected to scale as $\sigma_c(r) \propto r^{-1-\eta}$, where η is a critical exponent which turns out to be close to zero in most physical systems. A critical point would then correspond to a divergent Coulomb energy. As a consequence, the phase transition in stellar matter ends at a first-order point. This can be clearly seen in our numerical simulation as shown in Figure 6[20]. The critical point of the uncharged system is characterized by a diverging coulomb energy (upper right), while for the charged system at the end point of the coexistence zone (lower right) the fluctuation does not increase with the lattice size.

Such an effect has been already observed in Ising models with long-range frustrating interactions, where the coexistence region was seen to end at a first-order point [14]. Since the Fourier transform of the correlation function gives the enhancement of the in medium scattering cross section respect to its free value, the important physical implication of this result is that we expect hot stellar matter to show a small opacity to neutrino scattering[17], which may have important consequences on the cooling dynamics [22].

4. Conclusions

In this contribution we have estabilished some connections between exotic phases in stellar matter and nuclear multifragmentation. Both phenomena are triggered by an instability to finite wavelenght density fluctuations and can be understood in terms of frustration between the nuclear and the Coulomb interaction.

If the first order phase transition of normal nuclear matter is suppressed in stellar matter due to the high electron incompressibility, a (second order[6]) transition is however expected between single-phase and coexistence configurations. Large correlated structures are therefore predicted, even if at the ending point of the coexistence region the correlation lenght is not expected to diverge.

Since the Coulomb energy is minimized in homogeneous partitions corresponding to pure phases, and it is maximal in clusterized partitions, a higher temperature is needed to reach the mixed partitions with respect to the uncharged system. Therefore, the mixed-phase phenomenology may be relevant for the proto-neutron-star structure in a wider temperature range than usually expected [2]. Such an expansion of the coexistence region is at variance with the mean-field expectations . This contrast stresses the importance of realistic calculations beyond the mean-field level [16, 17].

Notes

a. Member of the Institut Universitaire de France

References

1. D.G.Yakovlev and C.J.Pethick, *Ann. Rev. Astron. Astroph.* **42** (2004) 169.
2. N.K.Glendenning, *Phys.Rep.* **342** (2001) 393.
3. D.Q.Lamb et al., *Nucl.Phys.* **A360** (1981) 459.
4. G.Bertsch, P.J.Siemens, *Phys. Lett.* **B 126** (1983) 9.
5. H.Muller and B.Serot, *Phys. Rev.* **C52** (1995) 2072.
6. Ph. Chomaz et al., arXiv:astro-ph/0507633 (2005).
7. C.Ducoin et al., in preparation.
8. E.Chabanat et al., *Nucl. Phys.* **A 627** (1997) 710.
9. F.Douchin, P.Haensel and J.Meyer, *Nucl. Phys.* **A665** (2000) 419.
10. J.M.Lattimer et al., *Nucl. Phys.* **A432** (1985) 646.
11. J.W.Negele and D.Vautherin, *Nucl.Phys.***A207** (1973) 298.
12. Since the density dependence of the neutron and proton effective mass is poorely known, we have used bare masses in this expression.
13. Conversely, charge neutrality affects the thermodynamics directly since it changes the number of degrees of freedom of the thermodynamic potentials.
14. M. Grousson, G. Tarjus and P. Viot, *Phys. Rev.* **E62** (2000) 7781; ibidem, *Phys. Rev.* **E64** (2001) 036109 .
15. D.G. Ravenhall, C.J. Pethick, J.R. Wilson, *Phys.Rev.Lett.* **50** (1983)2066 ; C.P. Lorenz, D.G. Ravenhall, C.J. Pethick *Phys.Rev.Lett.* **70** (1993)379 ; C.J. Pethick and D.G. Ravenhall, *Ann.Rev.Nucl.Part.Sci.* **45** (1995)429 .
16. G. Watanabe et al., *Phys. Rev.* **C69** 055805 (2004); ibidem, *Phys. Rev. Lett.* **94** 031101 (2005).
17. C.J. Horowitz, M.A. Perez-Garcia and J. Piekarewicz, *Phys. Rev.* **C69** 045804 (2004); C.J. Horowitz, and J. Piekarewicz, *Phys. Rev.* **C72** (2005) 035801.
18. F. Gulminelli et al., *Phys. Rev. Lett.* **91** 202701 (2003).
19. F. Gulminelli, *Ann.Phys.Fr.* (2005), in press.
20. P.Napolitani et al., in preparation.
21. P. Magierski and P.H. Heenen, *Phys. Rev.* **C65** 045804 (2001).
22. J. Margueron, J. Navarro and P. Blottiau, *Phys. Rev.* **C70** 28801 (2004).